PNAS
www.pnas.org

Supplementary Information for

Microtubule-directed transport of purine metabolons drives their cytosolic localization with mitochondria

Chung Yu Chan[a,b,1], Anthony M. Pedley[b,1], Doory Kim[c,1,2], Chenglong Xia[c], Xiaowei Zhuang[c,d,e,3], Stephen J. Benkovic[b,3]

[a]Department of Engineering Science and Mechanics, The Pennsylvania State University, University Park, PA 16802.
[b]Department of Chemistry, The Pennsylvania State University, University Park, PA 16802.
[c]Department of Chemistry and Chemical Biology, Harvard University, Cambridge, MA 02138.
[d]Howard Hughes Medical Institute, Harvard University, Cambridge, MA 02138.
[e]Department of Physics, Harvard University, Cambridge, MA 02138.
[1]These authors contributed equally.
[2]Present address: Department of Chemistry, Hanyang University, Seoul, South Korea, 133-791

[3]To whom correspondence should be addressed: zhuang@chemistry.harvard.edu (X.Z.) and sjb1@psu.edu (S.J.B.)

This PDF file includes:

Supplementary materials and methods
Figs. S1 to S7
Captions for movies S1 to S5
References for SI reference citations

Other supplementary materials for this manuscript include the following:

Movies S1 to S5

www.pnas.org/cgi/doi/10.1073/pnas.1814042115

Supplementary Materials and Methods

Plasmids and antibodies. Plasmids encoding FGAMS-EGFP and FGAMS-mMaple3 were constructed as previously reported (1). All plasmids were sequence verified by Sanger sequencing. Commercially available rabbit monoclonal anti-Tom20 (sc-11415; Santa Cruz Biotechnology) and rat monoclonal anti-tubulin (ab6160; Abcam) antibodies were used for immunostaining in stochastic optical reconstruction microscopy (STORM).

Cell culture and transient transfection of mammalian cells. HPRT-deficient (LND) fibroblasts were provided by Dr. H. A. Jinnah (Emory University, Atlanta, GA) and maintained in Dulbecco's Modified Eagle Medium (DMEM) with 4.5 g/L glucose (15-013; Corning) supplemented with 2 mM glutamine (Gibco) and 15% (v/v) fetal bovine serum (Atlanta Biologicals) at 37 °C and 5% CO_2.

HPRT-deficient fibroblasts at ~90% confluency were harvested and washed once with 1X Dulbecco's phosphate buffered saline (D-PBS) (21-031-CV; Corning) prior to electroporation using a Neon Transfection System MPK5000 (Invitrogen). For each 10 µL reaction, 2 µg of plasmid was added to $2.5 – 3.0 \times 10^5$ cells suspended in R buffer, and electroporation was performed with a voltage of 1400 V, pulse width of 20 ms for 2 pulses. Post-electroporation, cells were transferred to 35-mm^2 glass-bottom plate (MatTek) with complete growth medium and allowed to recover for 12 h prior to cell fixation or live cell imaging as previously reported (1).

Stochastic optical reconstruction microscopy (STORM). The samples were imaged in an imaging buffer containing 100 mM mercaptoethylamine (MEA) and an oxygen scavenger system [5% glucose (wt/vol), 0.5 mg/ml glucose oxidase (Sigma-Aldrich), and 40 mg/ml catalase (C100-50MG; Sigma-Aldrich)] in PBS at pH 8.5, which has a refractive index of 1.34. STORM imaging was performed on a customized microscopic system as previously described (1). For all two-color STORM experiments, images were taken on an Olympus IX71 inverted optical microscope equipped with an Olympus UPlanSApo 100x 1.4 NA oil immersion objective. An 830 nm infra-red (IR) diode laser (LPS-830-FC; Thorlabs) was introduced in a separated objective-type TIRF path for maintaining the focus of the Z-direction during data acquisition. For the activation of the fluorescent protein or photoactivatable dye (mMaple3 and Alexa 647), a solid-state laser beam of 405 nm (Cube 405-100C; Coherent) was employed.

For two-color imaging of mMaple3 and Alexa 647, solid-state lasers of 561 nm (MPB Communications Inc) and 647 nm (2RU-VFL-P-1500-647; MPB Communications Inc) were used to excite mMaple3 and Alexa 647, respectively, after 405 nm laser activation. These laser lines were reflected by a customized polychroic mirror (zt405/488/561/640rpc; Chroma) into the objective. The fluorescence emissions from mMaple3 and Alexa 647 were separated by a 630-nm longpass dichroic mounted on a commercial beamsplitting device (Dual-View; Photometrics), filtered with two bandpass emission filters (FF01-607/70; Semrock and ET705/72m; Chroma) and detected on two different regions of an electron-multiplying charge- coupled device (EMCCD) camera (Ixon DU897; Andor Technology) at a frame rate of 60 Hz. For added measure, a double notch filter (NF01-568/647; Semrock) was placed before the Dual-View to block the two excitation laser lines.

STORM images were generated using similar methods as previously described (1). Briefly, the centroid position coordinates (x0 and y0) of individual fluorophores and the Gaussian widths (dx and dy) were identified using an elliptical Gaussian function; the width values (dx and dy) were in turned used to determine the z coordinates of the fluorophores as previously described (2). For registration of two-color images of mMaple3 and Alexa647, the two STORM images were aligned

by a 3rd order polynomial warping map in 3D obtained from calibration images of 100 nm Tetraspeck fluorescent beads.

High resolution confocal microscopy. Three-colors live cell imaging of FGAMS, microtubules and mitochondria was performed on a Nikon Eclipse TE2000 inverted microscope equipped with VisiTech Instantaneous Selective Illumination Microscopic system (VT-iSIM; BioVision) and ORCA-Flash 4.0 V2 Digital CMOS camera (C11440-22CU; Hamamatsu). This system has a resolution of ~ 125 nm in the *x-y* plane. Images were collected using 100X CFI Apochromat TIRF 1.4 N.A. oil immersion objective (Nikon) with a theoretical pixel size of 56.5 nm. FGAMS-GFP transfected HPRT-deficient fibroblasts were stained with both 1 μM MitoTracker Red (M7513; Invitrogen) for mitochondria and 1 μM Silicon Rhodamine Tubulin (CY-SC002; Cytoskeleton, Inc) for microtubules at 37ºC and 5% CO_2 for 30 mins. 10 μM of verapamil was also added to improve the staining of microtubules. During image acquisition, samples were excited using 488, 561 and 642 nm solid state laser lines sequentially with 500 ms exposure time to minimize spectrum crosstalk. For time-lapse imaging, three colors images were taken by the software MetaMorph at 5 s per frame for 100 frames. The imaging buffer was FluoroBrite DMEM (A1896701; Gibco) with ProLong antifade solution (P7481; Invitrogen).

Immunostaining for Stochastic optical reconstruction microscopy (STORM). A total of 3.0-4.0 x 10^4 LND fibroblast cells were transiently transfected with plasmids encoding FGAMS-mMaple3, plated on a 35-mm^2 glass-bottom plate (MatTek), and allowed to recover at 37 °C and 5% CO_2 for 12 h. Adherent cells were fixed with freshly prepared 3% (v/v) paraformaldehyde (Electron Microscopy Sciences) and 0.1% (v/v) glutaraldehyde (Electron Microscopy Sciences) in D-PBS for 15 min at room temperature (RT). Cells were then incubated with 1 mg/mL sodium borohydride solution for 5 min and blocked with 3% (w/v) bovine serum albumin (IgG-free; Jackson ImmunoResearch) and 0.2% (v/v) Triton X-100 in PBS for 60 min. Primary antibodies for Tom20 (1:500 dilution) and tubulin (1:500 dilution) were prepared in the same blocking buffer and the cells were incubated for 60 min at RT. After primary antibodies incubation, cells were washed with 0.2% (w/v) BSA and 0.05% (v/v) Triton X-100 in D-PBS for 3 times and incubated with secondary antibodies (either anti-rabbit or anti-Rat) conjugated to Alexa 647 for 60 min at RT. The samples were incubated again in 3% (v/v) paraformaldehyde and 0.1% (v/v) glutaraldehyde for 10 min, and then were stored at 4 ºC in D-PBS or imaged in imaging buffer immediately.

STORM colocalization analysis. Colocalization between purinosomes and other subcellular components (either mitochondria or microtubules) was analyzed using custom written Matlab code as described previously (1). High-resolution images (~25.6 nm per pixel) of 2D projections of 3D STORM images of purinosomes and mitochondria (or microtubules) were median-filtered and subjected to intensity thresholding by Otsu's thresholding algorithm. Object boundaries were dilated by 1 pixel using 8-point connectivity to account for rounding errors in boundary identification. The Euclidean distance between mitochondria (or microtubules)-containing pixels and purinosome-containing pixels was determined and then used to determine the overlap matrix. The positive colocalization was defined as the mitochondria (or microtubules)-purinosome pixel distances being 100 nm or less.

High resolution confocal colocalization analysis. Colocalization between purinosomes and other subcellular components (either mitochondria or microtubules) was analyzed using modified STORM colocalization analysis Matlab code as described above. Likewise, high-resolution images of purinosomes and mitochondria (or microtubules) were median-filtered and subjected to intensity thresholding by Otsu's thresholding algorithm. Positive colocalization was defined as the boundary-to-boundary distances being 250 nm or less (VT-iSIM resolution: ~125 nm in x-y plane).

Randomized colocalization analysis. In order to determine how significant the colocalization number was, the expected colocalization percentage value for a randomized purinosome distribution was also simulated using the existing STORM or VT-iSIM data. To randomize the purinosome distribution, the cell and nuclear boundary were defined and the centroid position of each identified purinosome in the above analysis was randomly assigned to a pixel location within defined cytoplasmic area while leaving all other shape and size parameters constant. The purinosome distribution in each individual original image was randomized and the mean value of colocalization from the 10 randomized distribution images were calculated to compare with the true mitochondria distribution of the original image. Statistical significance of the difference in colocalization observed in true STORM or VT-iSIM images and randomized images was determined using a paired t-test.

Image visualization and statistical trajectory analysis of the representative three-color images. All images collected were handled and processed by Fiji-ImageJ (NIH). For the trajectory analysis, the position of an individual purinosome in a series of time-lapse images was recorded by the "Manual Tracking" plug-in in Fuji. The x and y positions (in terms of pixels) of the purinosome were recorded and converted into trajectory of x-y coordinates. Time-averaged Mean Square Displacement (MSD) for each trajectory was computed from the x-y coordinates prior to MSD fitting (3). Purinosomes of the respective colocalization categories were randomly selected across 30 representative cells.

Fitting of the time-averaged Mean Square Displacement (MSD). The time-averaged MSD $\langle r^2 \rangle$ was defined as the average of the squared displacements between the initial and final position of a purinosome in two dimensions of certain interval Δt for all time t within one trajectory. All trajectories were subject to MSD fitting in GraphPad as previously reported (4) with $R^2 > 0.97$ as the confidence level to determine the type of motion they represented.

In normal diffusion, $\langle r^2 \rangle$ of a purinosome is fitted with a linear equation as $\langle r^2 \rangle = 4D\Delta t$ where D is the diffusion coefficient. For the confined motion, $\langle r^2 \rangle$ of a purinosome is fitted with the equation as $\langle r^2 \rangle = \langle r_c^2 \rangle [1 - A_1 \exp(-4A_2 D\Delta t / \langle r_c^2 \rangle)]$ where $\langle r_c^2 \rangle$ represents the plateau value of $\langle r^2 \rangle$ in the MSD curve. Lastly, $\langle r^2 \rangle$ of a purinosome in directed motion is fitted with a quadratic equation $\langle r^2 \rangle = v^2\Delta t^2 + 4D\Delta t$ where v is the mean velocity of the trajectory.

Nocodazole treatment experiment. FGAMS-GFP transfected HPRT-deficient fibroblasts were incubated with 50 μM nocodazole (M1404; Sigma) in DMEM cell culture medium (as stated above) at 37 °C and 5% CO_2 for up to 3 h. After initial incubation, the cells were stained with 1 μM MitoTracker Deep Red in the same cell culture medium with nocodazole for 1 min. Prior to the imaging experiment, the cell culture medium was exchanged with imaging buffer (as stated above) and time-lapse two colors (FGAMS and mitochondria) imaging was carried out by VT-iSIM.

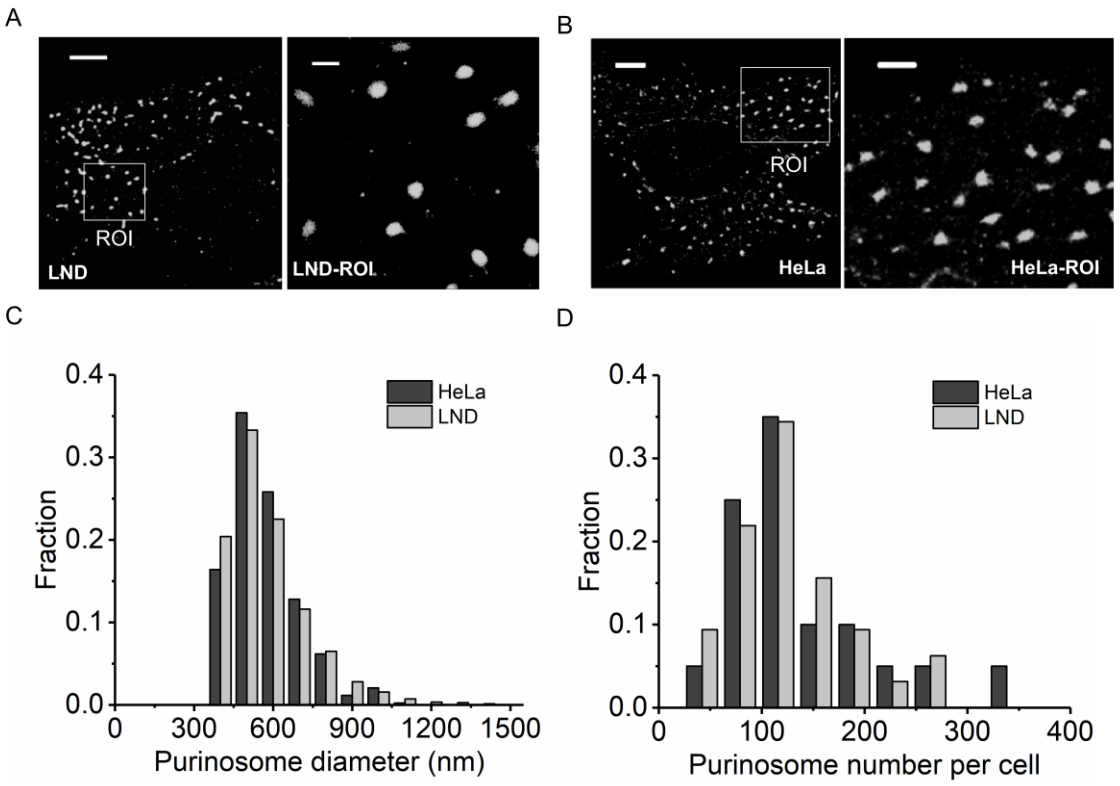

Fig. S1. Average diameter and density distributions of purinosomes in HPRT-deficient fibroblasts compared to purine-depleted HeLa cells by STORM. STORM images showing purinosomes as denoted by FGAMS-mMaple3 and the magnified ROIs in (A) HPRT-deficient (LND) fibroblasts and (B) purine-depleted HeLa cells. Scale bars = 5 μm (left panel) and 1 μm (right panel). (C) Comparison of the diameter of purinosomes in HeLa cells (black) and LND fibroblasts (gray). (D) Comparison of the density of purinosomes in a given HeLa cell (black) and LND fibroblast (gray). No significant differences in a purinosome's average diameter and density were observed between the two cell types.

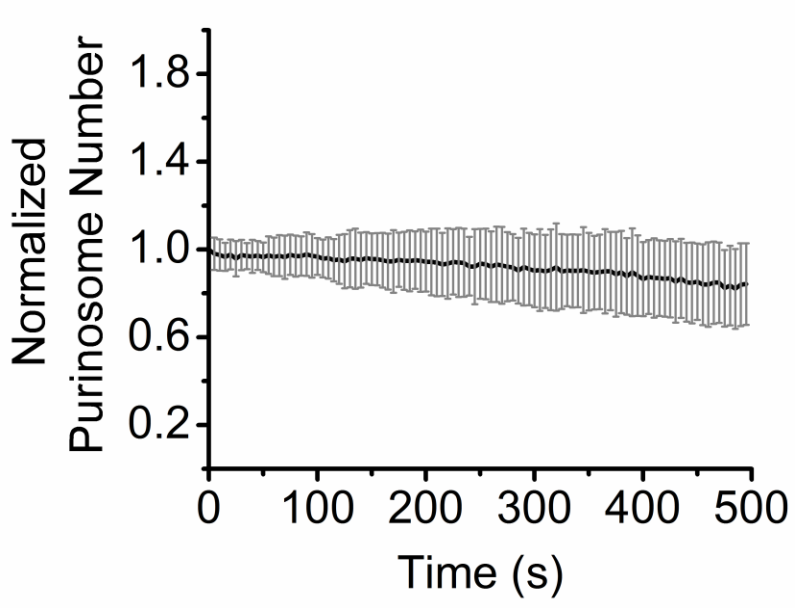

Fig. S2. Statistical analysis of the normalized number of purinosomes per cell over 495 s. The solid black line is the average normalized purinosome number showing the average purinosome number per cell did not change significantly over 495 s. Data are presented as mean ± S.D., N = 30 cells from 4 independent experiments.

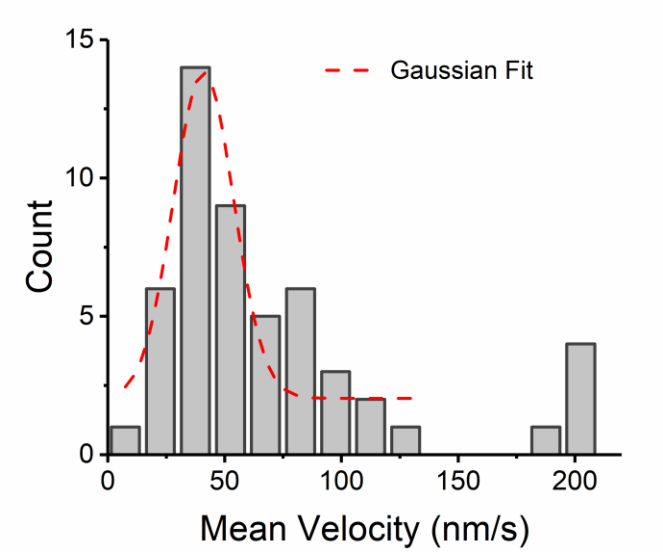

Fig. S3. A histogram of the mean velocity from MSD fitting of the directed motions. The median value is 55.2 nm/s for the mean velocity of directed motion. Data are presented as accumulated count, $N = 50$ representative trajectories.

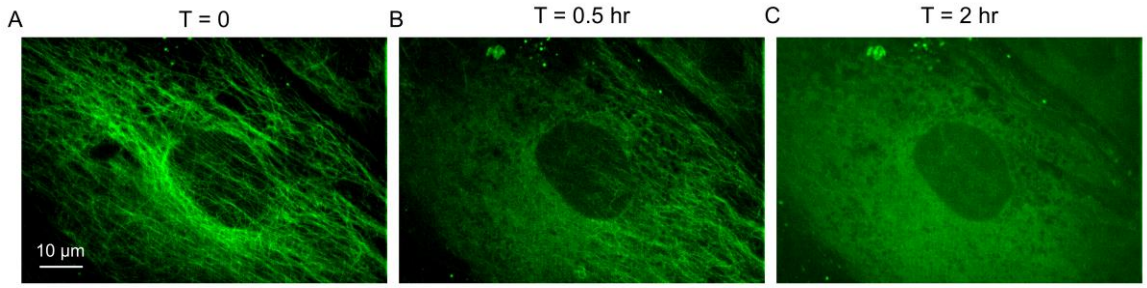

Fig. S4. Effect of nocodazole treatment on microtubules in HPRT-deficient fibroblasts. Representative time-lapse images of microtubules (green) as a function of nocodazole exposure: (A) Prior to treatment with nocodazole, (B) 0.5 h after nocodazole treatment, and (C) 2 h after nocodazole treatment. Complete depolymerization of microtubules were noted after 2 h of nocodazole treatment.

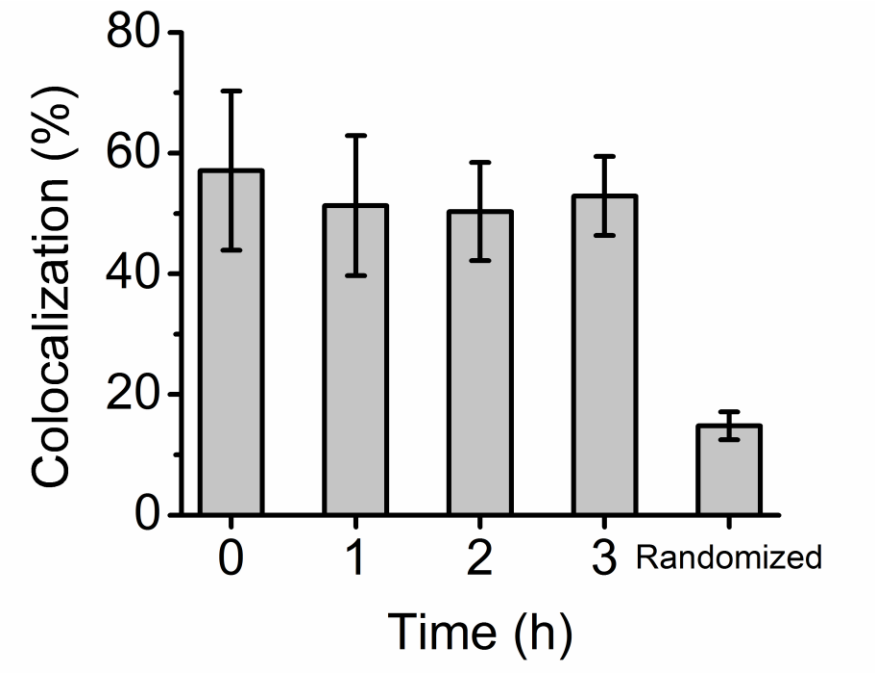

Fig. S5. Purinosome-mitochondria colocalization percentage as a function of time post-DMSO treatment, shown together with the randomization control results. Data are presented as mean ± S.D., N = 30 cells.

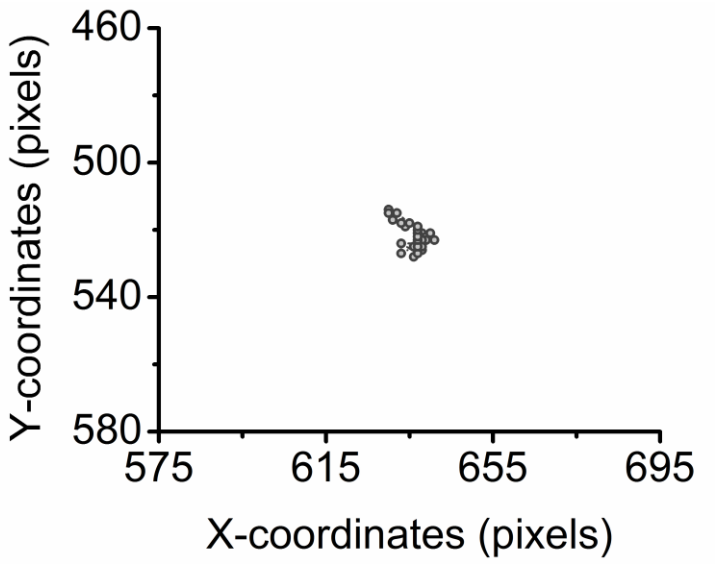

Fig. S6. Trajectory of the specified purinosome (white arrow) from (Fig. 4B) in *x*-*y* coordinates. This purinosome displayed random motion with minimal displacement.

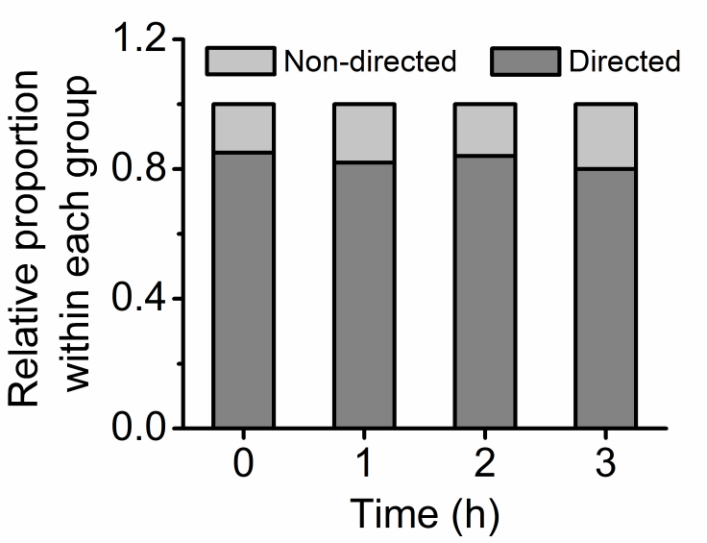

Fig. S7. Relative proportion of trajectories that displayed directed or non-directed motions as a function of time post-DMSO treatment. Only the trajectories of purinosomes not colocalized with mitochondria (- mito) were analyzed. N = 50 representative trajectories for each time point.

Movie S1. Interplay of purinosomes, mitochondria and microtubules over a 495 s time course.

Movie S2. Purinosome displaying minimal displacement while colocalized with both mitochondrion and microtubule.

Movie S3. Purinosome moving along a microtubule towards a mitochondrion.

Movie S4. Purinosome showing relatively small displacement while not colocalized with either mitochondrion or microtubule.

Movie S5. Motion of purinosomes after 3 h of nocodazole treatment.

References

1. French JB, *et al.* (2016) Spatial colocalization and functional link of purinosomes with mitochondria. *Science* 351(6274):733-737.
2. Huang B, Wang WQ, Bates M, & Zhuang X (2008) Three-dimensional super-resolution imaging by stochastic optical reconstruction microscopy. *Science* 319(5864):810-813.
3. Huang F, Watson E, Dempsey C, & Suh J (2013) Real-time particle tracking for studying intracellular trafficking of pharmaceutical nanocarriers. *Methods Mol Biol* 991:211-223.
4. de Bruin K, *et al.* (2007) Cellular dynamics of EGF receptor-targeted synthetic viruses. *Mol Ther* 15(7):1297-1305.